International Journal of Psychophysiology 157 (2020) 42–50

Contents lists available at ScienceDirect

International Journal of Psychophysiology

journal homepage: www.elsevier.com/locate/ijpsycho

Inflammation but not programmed cell death is activated in methamphetamine-dependent patients: Relevance to the brain function

Nooshin Ghavidel [a,b], Fariba Khodagholi [b], Abolhassan Ahmadiani [b], Reza Khosrowabadi [c], Sareh Asadi [d,*], Jamal Shams [e,**]

[a] Social Determinants of Health Research Center, Alborz University of Medical Sciences, Karaj, Iran
[b] Neuroscience Research Center, Shahid Beheshti University of Medical Sciences, Tehran, Iran
[c] Institute for Cognitive and Brain Sciences, Shahid Beheshti University, Tehran, Iran
[d] NeuroBiology Research Center, Shahid Beheshti University of Medical Sciences, Tehran, Iran
[e] Behavioral Research Center, Shahid Beheshti University of Medical Science, Tehran, Iran

ARTICLE INFO

Keywords:
Circulating markers
fMRI
MicroRNA
MBP
Stroop task
TNFα

ABSTRACT

Animal studies have shown that methamphetamine (MA) induces neurodegeneration through programmed cell death, however, the effects of MA on human brain and the extent of induced neural degeneration is not well understood. Given that the dose and duration of MA administration differ in animals and humans, we evaluated MA effects on active users considering brain damage mechanisms. Nineteen active MA-dependent patients and 18 healthy controls performed the color-word Stroop task, during fMRI and their blood samples were collected. Human enzyme-linked immunosorbent assays (ELISA) and quantitative PCR were applied to measure circulating proteins and miRNAs involved in various programmed cell death pathways (apoptosis, necroptosis, and autophagy), brain damage and neuroinflammation. Results showed the performance deficit in color-word Stroop task in MA abusers as well as higher activations of the right inferior and middle temporal gyri detected by fMRI. Structural MRI revealed increased white matter volume in MA-dependent patients in the superior and medial frontal gyri, and left/right middle temporal gyrus. Molecular analyses detected no significant differences in the plasma levels of the studied proteins and miRNAs of MA-dependent patients and controls except the higher levels of MBP, S100B, and TNFα in MA abusers. Results showed that MA induced physiological and structural changes accompanied by inflammation and release of damage-associated molecules in MA-dependent patients.

1. Introduction

Methamphetamine (MA) use remains a significant public health problem worldwide which has no effective pharmacological treatment to date. MA is a cationic lipophilic molecule which can substitute for dopamine, noradrenaline, and serotonin in dopamine transporter (DAT), noradrenaline transporter (NET), serotonin transporter (SERT) and vesicular monoamine transporter-2 (VMAT-2), reverses their functions, redistributes monoamines from storage vesicles into cytosol and synapse, and stimulates postsynaptic monoamine receptors. Long time use of MA results in depletion of presynaptic dopamine (DA) stores, and DA release into the cytoplasm, where DA undergoes auto-oxidation, producing toxic metabolites, oxidative stress, and mitochondrial dysfunctions followed by irreversible loss of nerve terminals and neuronal death (Moratalla et al., 2017; Shin et al., 2018).

MA abuse has been linked to numerous cognitive deficits particularly impairment in executive memory, motor skills, episodic memory, and executive functions (e.g. mental flexibility, self-control) (Dean et al., 2013; Zhong et al., 2016). One of the executive functions is cognitive control. The Stroop task combined with fMRI evaluates regional brain functions related to cognitive control (Herd et al., 2006). Human imaging studies have shown the association of MA neurotoxic effects with MA-induced behavioral and cognitive changes (Huang et al., 2017; Moszczynska and Callan, 2017). Functional magnetic resonance

* Correspondence to: S. Asadi, NeuroBiology Research Center, Shahid Beheshti University of Medical Sciences, Evin, Daneshjoo Blvd, P.O. Box 19615-1178, Tehran, Iran.
** Correspondence to: J. Shams, Behavioral Research Center, Imam Hossain Educational Hospital, Shahid Beheshti University of Medical Sciences, Madani Ave, P.O. Box 1617763141, Tehran, Iran.
E-mail addresses: s.asadi@sbmu.ac.ir (S. Asadi), J_shams@sbmu.ac.ir (J. Shams).

https://doi.org/10.1016/j.ijpsycho.2020.09.004
Received 31 October 2019; Received in revised form 31 May 2020; Accepted 11 September 2020
Available online 23 September 2020

imaging (fMRI) investigations have detected impairments in the MA abusers' prefrontal and striatal activation during experiments testing executive functioning (London et al., 2015; Nestor et al., 2011; Salo et al., 2009). Damage to both gray and white matter tissue within the frontostriatal regions of the MA-dependent patients' brain has been reported in the structural MRI studies (London et al., 2015).

Animal studies have shown that MA induces neuronal degeneration and cell death through all types of programmed cell death (PCD) mechanisms including apoptosis, autophagia and necroptosis (Davidson et al., 2001; Yu et al., 2015). MA induces apoptosis by enhancing in caspase-3 activity and the Fas/FasL cell death pathways (Jayanthi et al., 2005), as well as upregulation of endoplasmic reticulum (ER) stress-specific molecule caspase-12 (Xiao et al., 2018). A number of studies reported autophagy (Larsen et al., 2002) and necroptosis as the principal mechanisms of MA-induced cell injury (Xiong et al., 2016). Autophagia is associated with the appearance of autophagosomes and depends on the autophagy proteins. Increase micro tube-associated protein Light Chain (LC3), is considered as the main biochemical parameter for autophagy (Giménez-Xavier et al., 2008). Necroptosis is a programmed form of necrosis that can be induced by several molecular pathways and involves loss of plasma membrane integrity, organelle swelling, and leakage of intracellular contents. Mixed Lineage Kinase-Like pseudokinase (MLKL) mediates necroptosis (Berghe et al., 2014; Xiong et al., 2016).

Studies on progressive neurological disorders with brain damage in human have shown that some of the brain biochemical markers including specific neuronal enolase (NSE), protein S-100B, and myelin basic protein (MBP) are released to the systemic circulation possibly through the disturbed BBB (Lamers, 2003). MA also induces blood-brain barrier (BBB) disruption, but there is no study on circulating molecular markers of brain damage in MA-dependents.

MicroRNAs are short non-coding RNAs of about 20–22 nucleotides long that regulate gene expression by binding to the 3′-untranslated regions (3′-UTRs) of their mRNA targets. Most miRNAs act by down-regulating which target mRNA levels either by destabilization or degradation (Guo et al., 2010). Recently, studies have indicated that miRNAs are involved in substance use disorders, including alcohol, morphine, cocaine and MA addiction. Expression of microRNAs in the serum exosomes of MA-dependent rats has been detected and it has been observed that revealed MA changed miRNA profile (Li et al., 2018). Moreover, it has been reported that some miRNAs are decreased in the serum of MA-dependent patients (Zhao et al., 2016).

Although there are numerous animal studies showed that cell death was followed by MA abuse (Jayanthi et al., 2005; Xiao et al., 2018; Yu et al., 2015), the effects of MA on human brain and the extent of induced neural degeneration is not well understood. Most of the previous human studies investigating MA effects on human subjects used post mortem samples or imaging techniques. Post mortem studies showed reduced levels of three dopamine nerve terminal markers (Wilson et al., 1996; Worsley et al., 2000). Neuroimaging studies also demonstrated abnormalities in brain structure of MA-dependent patients (London et al., 2015).

Reports related to neurophysiological changes of human MA-dependents especially in active users are rare. There is little information about circulating molecular markers of cell death and brain damage in MA-dependents and their correlations with functional imaging measurements. Given that the dose and duration of MA administration differ in animals and humans, generalizing the results of animal studies to human MA addiction may be misleading. Moreover, the mechanism of MA-induced cell death in human brain is not still clear. Taken all together, we've hypothesized that the effects of MA on active users may be different with what has been reported in animal studies, so the purpose of this study was investigating the effects of MA on active MA abusers, specifically, cell death in MA-dependent patients and its relevance to the brain function. The study aim was investigated at different levels. Clinical and sociodemographic data was gathered through questioners. Circulating molecules (proteins and microRNAs) were measured to evaluate different mechanisms of cell death, brain damage, and inflammation in MA-dependent patients. Brain structure and its activity were studied through structural and functional MRI (combined with Stroop task for cognitive impairment evaluation). The correlations of the studied levels (clinical data, brain function as well as circulating proteins and miRNAs) were also investigated employing statistical methods.

2. Materials and methods

2.1. Subjects

The study sample consisted of two groups of Iranian male subjects recruited from September to December 2018, Tehran province: 21 MA-dependent patients from the substance abuse treatment programs and 19 normal controls. All of MA subjects were active users and did not have withdrawal time. Mean age and standard deviation of MA-dependent and controls were respectively 35.5 (±7.6) and 36.9 (±8.03). Group matching was based on age, gender, and education. Controls were selected from smokers without the history of substance use nor psychiatric disorders.

Inclusion criteria were defined as meeting DSM-5 criteria for MA dependence, age range between 20 and 50 years and the ability of reading and writing. The exclusion criteria were simultaneous use of other substance except for cigarette and methadone during the past four months which was checked by urine test (positive for MA and negative for other drugs), history of brain damage, serious psychiatric illness, suicide, brain surgery, neurological diseases, chronic disorders and contraindication for MRI.

This research was performed in accordance with the latest version of the Declaration of Helsinki and with the approval of the research ethics committee of Neuroscience Research Center, Shahid Beheshti University of Medical Sciences (IR.SBMU.MSP.REC.1396.319). Written consents for participation were obtained from the participants after being informed of the nature of the research.

2.2. Clinical assessments

Socio-demographic data was applied through a questionnaire consisting of the full name, age, weight, height, marital status, education, right/left handed. The Addiction Severity Index (ASI) questionnaire was used to determine medical status, drug use (the amount and duration of use), legal status, employment/support status, family/social and psychiatric status.

2.3. Color-word Stroop task

Stroop task (Stroop, 1935) measures selective attention, cognitive flexibility, and executive functions. The Stroop task stimuli consist of a random presentation of three color names (RED, BLUE and GREEN) in the congruent trials (e.g. the word RED displays in red ink) and the incongruent trials (e.g. the word "RED" displays in green ink) that were displayed through magnet-compatible goggles. Subjects were instructed to determine the color of words by pressing buttons on a device which was held by both hands. Subjects were trained before performing the task.

Each experiment consisted of 16 task blocks (eight congruent and eight incongruent trials) with 12 words per block (Helvetica font; 72 sizes; 6 mm × 15 mm) and 16 rest blocks with duration of 15 s which were white circles in the center of the screen. Stimuli were presented for 2000 ms with an interval of 500 ms (duration of each block was 30 s). Total task time was 12 min. Speed (reaction time) and accuracy (errors) of responses were measured.

2.4. Imaging

Functional and structural images were acquired on a 3 T Siemens (Prisma, Germany) head-only MRI scanner. T1 MPRAGE acquisition was collected for anatomical localization before the functional scanning session (echo time = 3.47 ms, repetition time = 1910 ms, voxel size 1 × 1 × 1 mˆ3, and flip angle = 7°). Following the T1 scan acquisition, a T2* weighted, gradient-recalled echo-echo planar imaging sequence was used for functional images (repetition time 3000 ms, 30 ms echo time, 90 degree flip angle, 46 slices, 3 mm slice thickness with a 3.0 mm slice spacing, image columns and rows 658 × 658, voxel size 2.5 × 2.5 × 2.5 mˆ3). During each run of the task, 240 brain volumes were collected. Scanning was fast event-related, with image acquisition synchronized to the stimulus onset.

Preprocessing fMRI analysis: First, we removed the 4 initial volumes (12 s) to reach the magnetic stability; then, data were preprocessed and analyzed using FMRIB Software Library (FSL 6.00) toolbox (https://fsl.fmrib.ox.ac.uk/fsl/fslwiki/). Image pre-processing steps were: high pass filtering slice timing correction, motion correction (head motion/rotation >3 mm) – normalization to Montreal Neurological Institute (MNI) space and finally spatial smoothing (in order to minimize residual differences in brain anatomy after spatial normalization).

2.5. Measurement of circulating molecular markers

Blood samples were collected from addicts and controls in EDTA anticoagulant collection tubes and were centrifuged for 15 min at 1500 ×*g* at 4 °C within 30 min of collection. Supernatants were collected to carry out molecular assays.

Human enzyme-linked immunosorbent assay (ELISA) kits were applied for the measurement of circulating molecular markers (BioTek Elisa reader, USA) including 1. Programmed cell death markers: caspase 3 for apoptosis (MyBioSource) - Mixed Lineage Kinase-Like pseudokinase (MLKL) for necroptosis (MyBioSource) and micro tube-associated protein 1A/1B Light Chain (LC3B) for autophagy (MyBioSource); 2. brain damage markers: S100 calcium-binding protein B (S100B) (MyBioSource) – myelin basic protein (MBP) (MyBioSource), Neuron-Specific Enolase (NSE) (MyBioSource) and 3. a neuro-inflammation marker: TNFα (MyBioSource) and analysis were done based on the manufacturer's protocol of kits.

2.6. Measurement of circulating microRNAs

Total microRNAs were extracted from plasma using miRNeasy Serum/Plasma Kit (Catalog No: 217184, Qiagen) according to the manufacturer's protocol in the presence of 20 microgram RNA carrier (Yeast RNA Purification Kit, Cat No: AM7120G, Ambion). To control the purification and cDNA synthesis efficiencies, prior to RNA isolation, 3.5 μl of synthetic miRNA-39 (cell-mir-39) (Catalog No: 219610, Qiagen) was added to the samples as a spike-in control. RNA quantity and integrity were determined by ND-2000 spectrophotometer (Thermo Fisher Scientific, Wilmington, DE, USA). To study the expression levels of miRNAs involved in programmed cell death, miR-15, miR-16, miR-let-7a were chosen for apoptosis (Su et al., 2015), miR-107 for necroptosis (Wang et al., 2015) and miR-181a for autophagy (Su et al., 2015). To evaluate the brain damage status miR-143 was also measured (Bai et al., 2016).

Complementary DNA was synthesized using the method that was described by Balcells et al. (2011). PCR primers were designed using the method proposed by Busk (2014). All reactions were performed in duplicate, and results were normalized to those for *C. elegans* miR-39. Relative expression levels of miRNA were determined by the delta delta CT method, where CT is the threshold cycle.

2.7. Statistical analysis

Statistical Analysis of fMRI imaging data: The analyses were performed using a General Linear Model (GLM). In the first-level analysis, individual subject GLMs were built and fitted to each subject's functional data based on congruent (C) and incongruent trials (IC) as well as Stroop effect (IC-C). For group analysis, two samples *t*-test using mixed effect was conducted. Age and the right/left handedness were included as covariates in the GLM models; the contrast images were thresholded. We used FSL default setting for correcting the multiple comparison. It uses GRF (Gaussian random field) method with a cluster P threshold of 0.05 and voxel Z threshold of 2.3 (Worsley, 2001).

A mask was built using the activated cluster in the inferior and middle temporal gyrus. Finally, the average level of activation of each subject was calculated in the defined mask. For structural images voxel-based morphometry (VBM) analysis was performed using SPM8 (Welcome Department of Imaging Neuroscience: http://www.fil.ion.ucl.ac.uk/spm).

Structural image preprocessing: Brain images were extracted and segmented into tissue probability maps (TPM) of gray matter, white matter, and cerebrospinal fluid, which were registered to MNI 152-space standard space. Gray matter TPMs were modulated with nonlinear warping parameters to account for local morphological differences and then were spatially smoothed with the full width at half maximum (FWHM) of 8 mm. Results were presented with the xjview toolbox (http://www.alivelearn.net/xjview).

Comparison of socio-demographic data, clinical variables, Stroop task factors, circulating biomarkers and miRNA expression levels between MA-dependent patients and controls were conducted by *t*-test (parametric) or Mann-Whitney test (non-parametric). Pearson and Spearman's tests as well as multiple linear regression analysis were also performed to evaluate the correlation of data. All probability values are two-sided, and a probability value less than 0.05 was considered statistically significant.

3. Results

3.1. Sample characteristics

Two MA abusers and one control subject were excluded from the study because of head motion/rotation and inappropriate MRI signals. Data of 19 MA-dependent patients and 18 controls were finally used for functional MRI and molecular evaluations. Socio-demographic data and drug use information have been shown in Table 1. Both groups were smokers but the number of cigarette use differed significantly.

3.2. Stroop task performance

The color-word Stroop task performance of subjects showed more incorrect responses in MA users than control subjects as well as significantly different Stroop effect in these two groups (Table 2) but there were no significant differences on reaction time indices.

There was no significant correlation between pattern of MA use (years and amount of MA use) and Stroop task performance.

Table 1
Demographic and drug use measures of 19 MA abusers and 18 control subjects.

Variables	Control subjects Mean (±SD)	MA abusers Mean (±SD)	P-value
Age, years	36.9 (±8.03)	35.5 (±7.6)	0.58
Educational level, years	8.5 (±4.5)	7.0 (±3.1)	0.24
Cigarette use, pack year	7.1 (±10.3)	13.1 (±8.1)	0.01*
Mean daily MA use, g	–	0.8 (±0.61)	
MA use duration, years	–	8.0 (±3.6)	
Age of first MA use, years	–	27.5 (±8.2)	

* Significantly different from the control group. $P < 0.05$.

Table 2
Stroop task results from 19 MA Abusers and 18 Control Subjects.

Stroop task performance	Control subjects Mean ± SEM	MA abusers Mean ± SEM	P-value
Total error	7.0 (±1.7)	33.5 (±10.3)	0.04*
Incongruent error	5.1 (±1.1)	21.7 (±5.9)	0.03*
Congruent error	1.9 (±0.7)	11.8 (±4.7)	0.14
Stroop effect	3.2 (±1.0)	9.8 (±2.7)	0.04*
Total RT	1.2 (±0.05)	1.2 (±0.06)	0.33
Congruent RT	1.1 (±0.05)	1.1 (±0.06)	0.76
Incongruent RT	1.3 (±0.05)	1.3 (±0.07)	0.99
Stroop effect RT	0.1(±0.02)	0.17 (±0.03)	0.57

RT, reaction time.
* Significantly different from the control group, $P < 0.05$.

3.3. Functional MRI

We performed *t*-test analyses between two groups to reveal group differences in the three conditions of interest (congruent, incongruent, and Stroop effect). Comparing the function of brain areas in MA-dependent patients and controls revealed no significant difference in congruent and incongruent conditions. In the Stroop effect condition of fMRI, both groups showed activations in frontal gyrus, anterior cingulate gyrus, occipital cortex, inferior temporal gyrus, and superior parietal lobe, but significant difference in the right inferior temporal gyrus was detected (threshold 2.3; P value = 0.05) (Fig. 1).

3.4. Structural MRI

VBM was conducted to evaluate the structural changes in subjects. Voxel-wise comparison of the two groups was performed in SPM8, using independent two-tailed t-test analysis. The significance level was set at the corrected P-value < 0.001 and family-wise error (FWE < 0.05) correction. Analysis showed increased white matter volume in MA-dependent patients relative to the controls in some areas including right superior temporal gyrus, left temporal lobe, right frontal lobe and left medial frontal gyrus (Fig. 2). Table 3 summarizes data for regions with significantly different white matter volume between the MA abusers and control subjects.

3.5. Circulating proteins levels

Comparing the levels of blood markers between MA-dependent patients and controls showed no significant differences for the proteins involved in programmed cell death including Caspase 3, MLKL and LC3B; however, levels of MBP, S100B and TNFα were significantly higher in MA abusers compared to the controls (P-values: 0.03, 0.02 and 0.03 respectively) (Table 4).

There was no significant correlation between pattern of MA use (years and amount of MA use) and plasma molecular markers.

3.6. Circulating microRNAs levels

Table 5 shows the levels of plasma miRNAs in the MA abusers and controls. Mann-Whitney test revealed no significant differences between miRNAs levels in these two groups.

There was no significant correlation between pattern of MA use (years and amount of MA use) and plasma microRNAs.

3.7. Correlation of imaging data, Stroop task and circulating biomarkers

A mask was built using the activated cluster in the right inferior and middle temporal gyri and the average level of activation of each subject

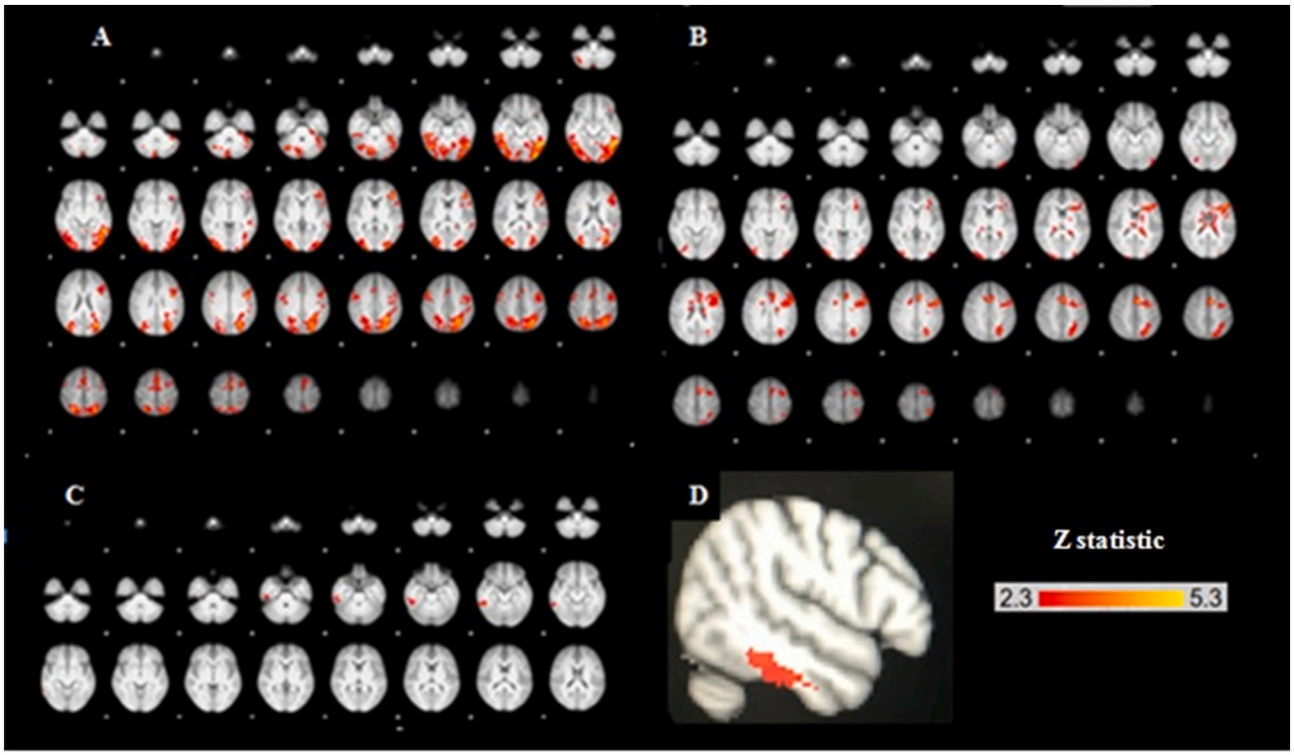

Fig. 1. Average Blood Oxygen Level Dependent (BOLD) activation for Stroop effect condition (IC-C) in MA abusers and control subjects following the performance of color-word Stroop task trials. (A) Average BOLD activation of MA abusers (N = 19); (B) average BOLD activation of control subjects (N = 18); (C) and (D) coronal and lateral views of brain activation, highlighted regions showed increased BOLD activity in MA abusers relative to the controls by using unpaired *t*-test analysis for the Stroop effect (high activation in right inferior temporal gyrus). Images were thresholded using clusters determined by Z > 2.3 and a corrected cluster significance level of P < 0.05. The scale represents the color (from dark to light yellow) of the cluster corresponding to the increasing Z-statistic. (For interpretation of the references to color in this figure legend, the reader is referred to the web version of this article.)

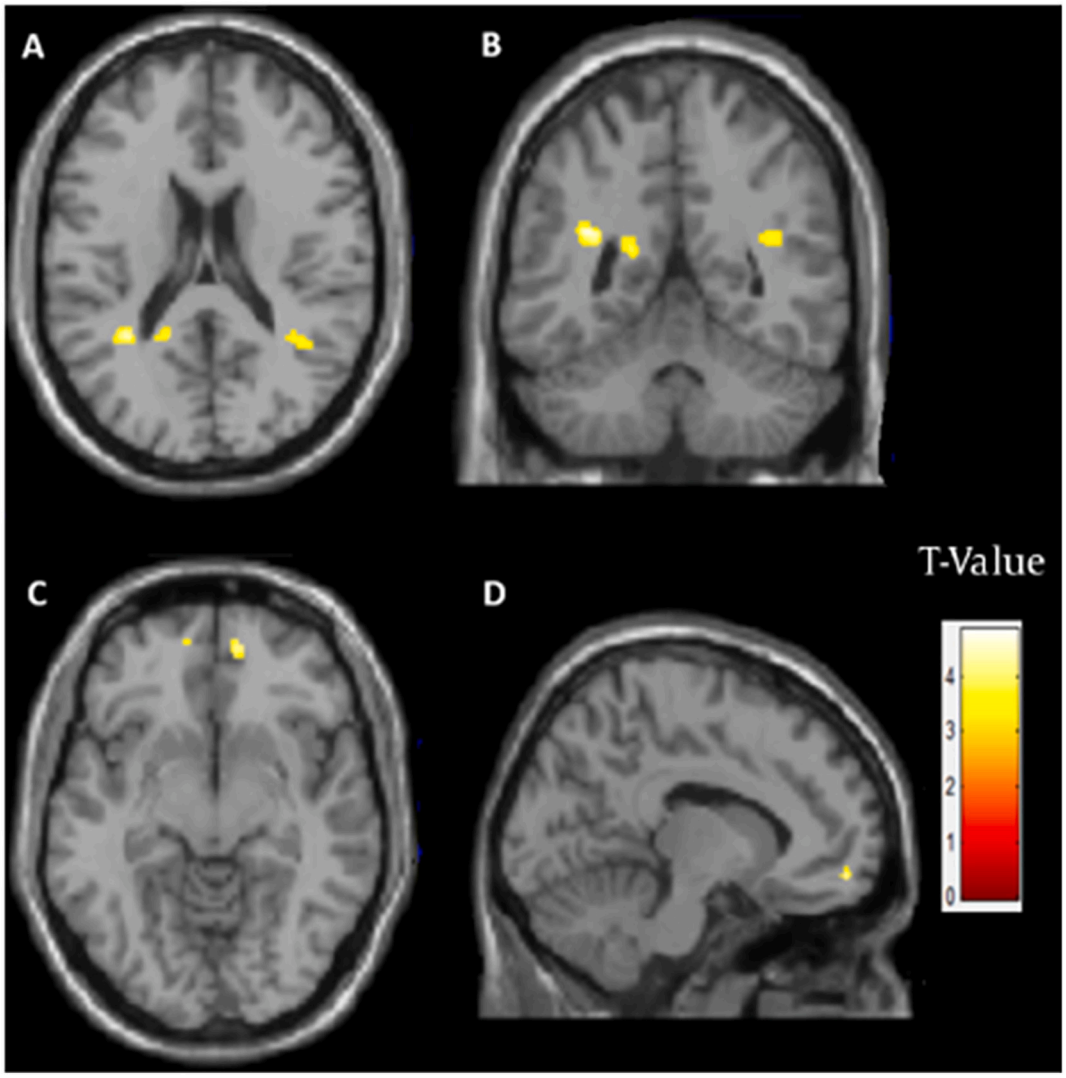

Fig. 2. Comparison of the structural MRI in MA abusers and control subjects using VBM and independent two-tailed t-test analysis. A, B. Transverse and coronal view of the brain, increased white matter volume in the right superior temporal gyrus (RSTG) and left temporal lobe (LTL) in MA-dependent patients relative to controls. C, D. Transverse and sagittal view of the brain, increased white matter volume in right frontal lobe sub-gyral and Left medial frontal gyrus in MA-dependent patients relative to the controls (P-value < 0.001 FWE < 0.05).

Table 3
Increased white matter volume of brain Regions volume in MA-dependent patients compared to controls in VBM.

Region	T-value	P-value	Cluster size	MNI coordinates		
				X	Y	Z
Right superior temporal gyrus	3.365	0.001	>5	42.12	−50.55	19.50
Left temporal lobe/sub-gyral	3.365	0.001	>5	−31.87	−49.41	19.50
Left/sub lobar/ extra-nuclear	3.365	0.001	>5	−17.08	−48.27	19.50
Right frontal lobe sub-gyral	3.365	0.001	>5	13.66	52.24	−8.18
Left medial frontal gyrus	3.365	0.001	>5	−10.25	53.38	−8.18

Table 4
Plasma molecular markers of 19 MA abusers and 18 control subjects.

Biomarkers	Control subjects Mean (±SEM)	MA abusers Mean (±SEM)	P-value
MBP* (pg/ml)	118.2(±9.0)	144.3(±9.7)	0.03*
NSE (ng/ml)	57.6 (±2.3)	53.2 (±2.2)	0.06
S100B* (pg/ml)	41.9 (±4.5)	60.5 (±6.0)	0.02*
TNFα* (pg/ml)	10.0 (±0.6)	11.3 (±0.5)	0.03*
Caspase3 (ng/ml)	19.36 (±0.03)	19.38 (±0.05)	0.78
MLKL (pg/ml)	193.0 (±22.6)	147.0 (±26.4)	0.07
LC3B (pg/ml)	22.15 (±1.9)	19.56 (±1.5)	0.29

* Significantly different from the control group, $P < 0.05$.

was calculated in the defined mask as fMRI results. Correlations of fMRI results, Stroop task performance, levels of circulating proteins and miRNAs were assessed using Pearson and Spearman correlation analyses for all of the studied subjects (both MA abusers and controls). Results showed a significant correlation between the function of brain areas (right inferior and middle temporal gyri) and incongruent (IC) error, Stroop effect, and plasma MBP levels, as well as between MBP and IC errors (Fig. 3).

Association between MBP, IC and Stroop effect with fMRI was also investigated using linear regression analysis (Table 6). fMRI activity as dependent variable; MBP, IC and Stroop effect as the predictor variables; age and smoking as covariates were considered in linear regression analysis. After multiple regression analysis (adjusted for age and

Table 5
Plasma microRNAs of 19 MA abusers and 18 control subjects.

MicroRNAs	Control subjects Mean (±SEM)	MA abusers Mean (±SEM)	P-value
miR-15	1.17 (±0.4)	1.58 (±0.4)	0.65
miR-16	1.09 (±0.3)	2.24 (±0.7)	0.19
miR-let-7a	1.33 (±0.4)	2.28 (±1.1)	0.82
miR 107	1.44 (±0.5)	2.11 (±0.9)	0.79
miR181a	1.09 (±0.4)	2.26 (±0.8)	0.32
miR143	1.11 (±0.3)	2.78 (±1.3)	0.95

Data presented as fold of changes.

smoking), significantly correlations between MBP, IC and Stroop effect with fMRI were observed.

4. Discussion

Results of the current study detected performance deficit in the color-word Stroop task and higher activation of right inferior temporal gyrus in MA abusers compared to the control subjects as well as the increased white matter volume in MA-dependent patients in the right superior temporal gyrus, left temporal lobe, right frontal lobe and left medial frontal gyrus. Molecular analyses detected significantly higher MBP, S100B, and TNFα plasma levels in MA abusers compared to controls but the levels of the circulating markers including plasma proteins (caspase 3, MLKL, and LC3B) and miRNAs (miR-15, miR-16, let-7a, miR-103, miR-107, miR-181a, and miR-143) involved in various programmed cell death mechanisms (apoptosis, necroptosis and autophagy) were not significantly different in MA abusers and control subjects.

4.1. Deficit in the color-word Stroop task and brain imaging analyses

MA induces various aberrant changes in human brain including neuropsychiatric disturbances, cognitive impairment and neurodegenerative changes (Gold et al., 2009). Studies demonstrated that MA abuse is associated with physiologic changes in the brain which are accompanied by the slower reaction times of cognitive function (Chang et al., 2002). Previous fMRI investigations have shown that MA users have impairments in striatal and prefrontal activation during tests of executive functioning (London et al., 2015). Findings of the current study also detected impaired performance in Stroop task in MA abusers that was consistent with results of the previous investigations reporting cognitive impairment in active MA abusers (L. Simon et al., 2000), recently abstinent (Nestor et al., 2011) and long-term abstinent MA abusers (Salo et al., 2009). Performance deficit in Stroop task may be related to the

Table 6
Association between MBP, IC and Stroop effect with fMRI: Linear regression analysis.

	B (SE)	β	P	B (SE)[a]	β	P
MBP	0.010 (0.004)	0.40*	0.016	0.010 (0.004)	0.40*	0.021
IC	0.018 (0.007)	0.41*	0.014	0.020 (0.008)	0.45*	0.012
Stroop effect	0.043 (0.015)	0.44*	0.008	0.46 (0.016)	0.47*	0.007

Dependent variable: fMRI.
B: unstandardized coefficients.
β: standardized coefficients.
* $P < 0.05$ indicates statistically significant difference.
[a] Adjusted for smoking and age.

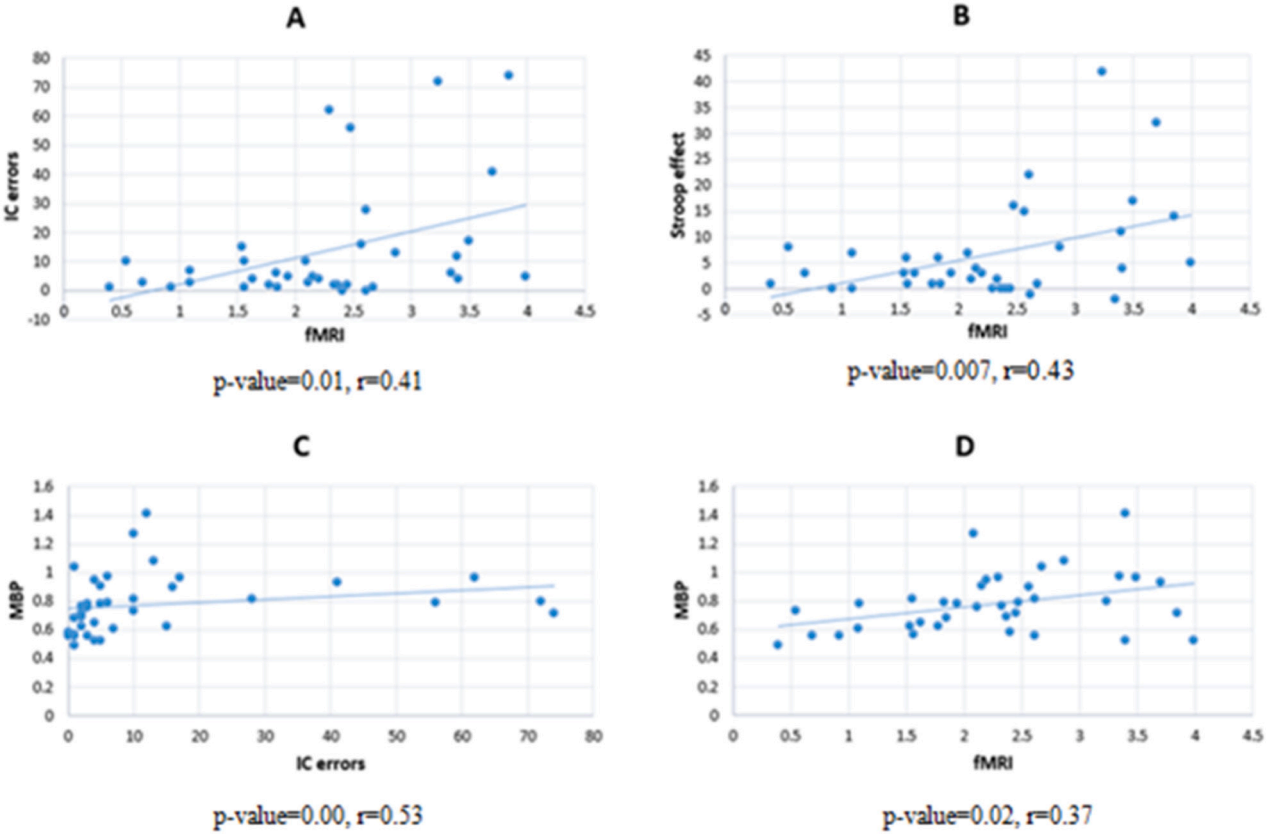

Fig. 3. Correlation scatters plots of some covariates in all subjects (MA abusers and control subjects); (A) correlation between fMRI and IC error; (B) correlation of fMRI and Stroop effect (IC-C); (C) correlation of MBP and IC errors; (D) correlation of MBP and fMRI. IC = incongruent, MBP = myelin basic protein.

impaired ability to suppress irrelevant information and impaired executive function which is important for suppressing habitual behaviors in MA abusers. Consistent with the results of Fassbender et al. (2015), we also found no significant correlation between task performance and MA use pattern (dosage, years of use, the age of first MA use) in MA abusers. However, the impaired performance in the Stroop task was correlated with higher activation of the right inferior and middle temporal gyrus of MA abusers in the present study. This area is one of the dorsal attention network (DAN). DAN is related to externally oriented attention and is typically activated during cognitive tasks requiring external attention (Krebs et al., 2012). It is proposed that MA abusers recruited additional attention regions during the Stroop task but because of neuronal damage in their frontocingulate cortex which is important in conflict resolution; their error rates were significantly higher than control groups.

Previous studies which investigated the effects of MA on the structure of the human brain reported smaller cortical but larger striatal gray-matter volumes in MA-dependent patients compared to the controls (London et al., 2015). More years of MA use negatively correlated with GMV in the right superior frontal and temporal gyri and the right caudate nucleus (Ruan et al., 2018). Thompson et al. showed severe gray-matter deficits in the cingulate, limbic, and paralimbic cortices of MA abusers as well as smaller hippocampal volumes than control subjects and significant white-matter hypertrophy which were correlated with memory performance on a word-recall test (Thompson et al., 2004). Results of the present study showed increased white matter volume in some of the MA addicts' brain areas including right superior temporal gyrus, left temporal lobe, right frontal lobe and left medial frontal gyrus compared to the controls. The observed structural changes were not compatible with functional impairments detected by fMRI; however, white matter enlargement may reflect the compensatory response due to the involvement of inflammation, axon and myelin damage or microgliosis secondary to neuronal damage following MA consumption (Thompson et al., 2004). This hypothesis is consistent with in vitro findings that MA might induce inflammation by stimulating the increased release and/or activation of matrix-degrading proteinases (Conant et al., 2004). We also observed higher plasma TNFα, S100B, and MBP in the plasma of MA abusers compared to controls supporting this hypothesis.

4.2. Circulating proteins

4.2.1. TNFα

TNFα is produced in CNS by microglia and astrocytes in response to pathological processes, including infection, inflammatory disease, ischemia, and traumatic injury (Feuerstein et al., 1994). Elevated serum and tissue levels were reported in inflammatory and infectious condition (Bradley, 2008). Gonçalves et al. reported increased expression levels of TNFα in the hippocampus and frontal cortex of mice 30 min post-MA administration (Gonçalves et al., 2008). PET human and animal studies also demonstrated that MA induces microglia and astroglia activation (Moratalla et al., 2017; Sekine et al., 2008), resulted in elevated TNFα plasma. We also detected higher TNFα levels in MA abusers showing inflammation and glial activation in these patients.

4.2.2. S100B

The presence of S100B in serum is an early marker of BBB openings that may precede neuronal damage (Marchi et al., 2003). S100β is a calcium-binding protein produced and released by glial cells especially astrocytes in the central nervous system (CNS). It has various intracellular functions such as regulation of protein phosphorylation, cytoskeleton composition, calcium homeostasis, and cell proliferation and differentiation. Extracellular functions of S100B are trophic and toxic effects on neuroglial cells at nanomolar and micromolar levels, respectively (Sen and Belli, 2007). Previous studies showed elevated circulating S-100B in stroke, head injury, brain tumor, cardiopulmonary bypass surgery, cardiac arrest (Lamers, 2003) and synthetic cannabinoid use disorder (Yilmaz et al., 2018). We also detected S100B levels less than the nanomolar range which may correlate with glial proliferation but not cell death.

4.2.3. MBP

MBP is the second most abundant protein of myelin sheath in the CNS and responsible for adhesion of the cytosolic surfaces of multilayered compact myelin (Zhang et al., 2014). MBP was reported to induce glial activation, bind to the extracellular surface of the neuronal plasma membrane, and induce neurotoxicity in vitro (Zhang et al., 2014). MBP has been detected in blood circulation in head injury (Yamazaki et al., 1995) and multiple sclerosis (Ohta et al., 2002). Cohen et al. proposed that MBP in cerebral spinal fluid (CSF) appears to be a useful index of active demyelination (Cohen et al., 1976). In the heroin-induced spongiform leukoencephalopathy (HSLE) patients have found collapse and fracture of myelin sheaths and vacuole formation in the sub-cortical white matter as well as increased CSF MBP (Yin et al., 2013). The observed higher level of MBP in the current study and its correlation with incongruent errors and inferior temporal cluster function suggests that MA-induced myelin damage followed by reduced speed of neuronal conduction and executive function deficits detected by fMRI.

4.2.4. Cell death markers

A body of literature on the MA-induced cell death in animal studies exists which have revealed neuronal death in MA administration (Jayanthi et al., 2005; Xiao et al., 2018; Xiong et al., 2016), but MA effects on the structure and chemistry of human brain has not been well understood. Positron emission tomography (PET) investigations have demonstrated that compared to the control subjects, MA abusers exhibit reduced levels of dopamine transporters in the prefrontal cortex and striatum (Sekine et al., 2003), alterations in cerebral perfusion (Chang et al., 2002), levels of neuronal metabolites (Ernst et al., 2000), and brain structural deficits (Thompson et al., 2004). The results of PET studies are consistent with the findings from postmortem investigations reported the reduced level of DAT in the basal ganglia of MA abusers (Wilson et al., 1996).

To answer the question whether MA in the human brain induced neuronal death similar to findings of animal studies, we evaluated circulating proteins involved in the various programmed cell death pathways including apoptosis (caspase3), necroptosis (MLKL) and autophagia (LC3B). Our observations did not detect significant differences between MA abusers and control subjects in none of the studied markers.

4.3. Circulating miRNAs

Other modulators of addictive drugs are miRNAs that are mediating the expression of target genes in nicotine, cocaine, opioid and alcohol addiction (Li et al., 2018). Studies investigating the regulatory role of miRNAs in MA addiction are limited but it has been shown that MA can induce changes in miRNA expression levels. Zhao et al. found that the expression of miR-181a, miR-15b, miR-let-7e, miR-let-7d in plasma of MA-dependent patients were decreased compared to the controls and this alteration was negatively correlated with drug use frequencies in past months (Zhao et al., 2016). Moreover, it has been shown that miR-15, miR-16, and miR-let-7a were involved in apoptosis (Su et al., 2015), miR-107 in necroptosis (Wang et al., 2015), and miR-181a in autophagy (Su et al., 2015). However, the results of the current study detected no significant differences in these five miRNAs between MA-dependent patients and controls, but their levels were generally higher in MA group. Human studies with larger samples will need to be performed in the future to verify significant differences of these miRNAs between the MA and control groups.

We also evaluated circulating miR-143 to assess brain effects of MA. Results showed that miR-143 was not significantly differed between these two groups. Bai, Zhang, and colleagues have shown that silencing

miR-143 in a genetic animal model or via an anti-miR-143 lentivirus protected the BBB integrity against the effects of MA. They also found a significant increase in the level of miR-143 in the serum of MA abusers compared to the healthy controls (Bai et al., 2016).

There are animal studies reporting MA-induces neurite degeneration without cell bodies destruction (Larsen et al., 2002). Pubill et al. also found that MA-induced 35% loss of dopaminergic terminals, generally without cell death, and astrogliosis in the striatum, cortex, and hippocampus of the rat brain (Pubill et al., 2003). So, they hypothesized that MA induces an unusual type of neurodegeneration in which axonal damage of dopaminergic neurons happens without affecting cell bodies. Results of the current study may provide further evidence for these reports as we've detected increased levels of plasma MBP, S100B and TNFα as neuronal damage and inflammatory factors.

This study had some limitations which the first one was the small sample size, so replication of this study with a larger sample is required. Second, the control group was significantly differed with patient group in cigarette use. Replication of this study with control subjects who smoke more (about 13.1 ± 8.1 (mean $\pm$ SD) pack cigarette per year) may help to relate the observed data to MA vs cigarette use. Finally, without some form of genetic controls, it is not possible to claim on the effect of MA on the obtained results; albeit comparing MA-dependent patient group with the control group allowed us to suggest causal effects of MA which need more verifications. To verify whether these observed neural effects in the current study, were pre-existing or due to MA usage, further studies with genetic controls will need to be performed in future.

5. Conclusion

In conclusion, detected performance deficit in the Stoop task along with the higher activation of right inferior temporal gyrus, white matter hypertrophy, inflammation and release of damage-associated molecules in MA-dependents proposed MA-induced physiological and structural changes without activation of apoptosis, necroptosis, or autophagy. To verify these results, human studies with larger samples and more comprehensive investigations will need to be performed in future.

CRediT authorship contribution statement

NG, FK, AA, SA, and JS contributed to the concept and design of the study. NG and SA contributed to the literature search, data analysis, interpretation of findings and manuscript preparation. NG was responsible for the acquisition of clinical data including imaging data and molecular experiments as well as statistical analysis. RK contributed to the design of imaging experiments, analysis of imaging results and their interpretation. All authors critically reviewed content and approved the final version for publication.

Declaration of competing interest

Authors declared no conflict of interest.

Acknowledgments

This article has been extracted from the thesis written by Nooshin Ghavidel in School of Medicine, Shahid Beheshti University of Medical Sciences (Registration No: 79). This study was supported by Neuroscience Research Center, Shahid Beheshti University of Medical Sciences, Iran; and Iran National Science Foundation (Grant no. 96015957). We greatly appreciate the collaboration of National Brain Mapping Lab, Tehran, Iran for providing data recording services.

References

Bai, Y., Zhang, Y., Hua, J., Yang, X., Zhang, X., Duan, M., Zhou, R., 2016. Silencing microRNA-143 protects the integrity of the blood-brain barrier: implications for methamphetamine abuse. Scientific reports 6, 35642.
Balcells, I., Cirera, S., Busk, P.K., 2011. Specific and sensitive quantitative RT-PCR of miRNAs with DNA primers. BMC Biotechnol. 11 (1), 70.
Berghe, T.V., Linkermann, A., Jouan-Lanhouet, S., Walczak, H., Vandenabeele, P., 2014. Regulated necrosis: the expanding network of non-apoptotic cell death pathways. Nat. Rev. Mol. Cell Biol. 15 (2), 135.
Bradley, J., 2008. TNF-mediated inflammatory disease. J. Pathol. 214 (2), 149–160.
Busk, P.K., 2014. A tool for design of primers for microRNA-specific quantitative RT-qPCR. BMC Bioinforma. 15 (1), 29.
Chang, L., Ernst, T., Speck, O., Patel, H., DeSilva, M., Leonido-Yee, M., Miller, E.N., 2002. Perfusion MRI and computerized cognitive test abnormalities in abstinent methamphetamine users. Psychiatry Res. Neuroimaging 114 (2), 65–79.
Cohen, S.R., Herndon, R.M., McKhann, G.M., 1976. Radioimmunoassay of myelin basic protein in spinal fluid: an index of active demyelination. N. Engl. J. Med. 295 (26), 1455–1457.
Conant, K., Hillaire, C.S., Anderson, C., Galey, D., Wang, J., Nath, A., 2004. Human immunodeficiency virus type 1 Tat and methamphetamine affect the release and activation of matrix-degrading proteinases. J. Neurovirol. 10 (1), 21–28.
Davidson, C., Gow, A.J., Lee, T.H., Ellinwood, E.H., 2001. Methamphetamine neurotoxicity: necrotic and apoptotic mechanisms and relevance to human abuse and treatment. Brain Res. Rev. 36 (1), 1–22.
Dean, A.C., Groman, S.M., Morales, A.M., London, E.D., 2013. An evaluation of the evidence that methamphetamine abuse causes cognitive decline in humans. Neuropsychopharmacology 38 (2), 259.
Ernst, T., Chang, L., Leonido–Yee, M., Speck, O., 2000. Evidence for long-term neurotoxicity associated with methamphetamine abuse: a 1H MRS study. Neurology 54 (6), 1344–1349.
Fassbender, C., Lesh, T.A., Ursu, S., Salo, R., 2015. Reaction time variability and related brain activity in methamphetamine psychosis. Biol. Psychiatry 77 (5), 465–474.
Feuerstein, G., Liu, T., Barone, F., 1994. Cytokines, inflammation, and brain injury: role of tumor necrosis factor-alpha. Cerebrovasc. Brain Metab. Rev. 6 (4), 341–360.
Giménez-Xavier, P., Francisco, R., Platini, F., Pérez, R., Ambrosio, S., 2008. LC3-I conversion to LC3-II does not necessarily result in complete autophagy. Int. J. Mol. Med. 22 (6), 781–785.
Gold, M.S., Kobeissy, F.H., Wang, K.K., Merlo, L.J., Bruijnzeel, A.W., Krasnova, I.N., Cadet, J.L., 2009. Methamphetamine-and trauma-induced brain injuries: comparative cellular and molecular neurobiological substrates. Biol. Psychiatry 66 (2), 118–127.
Gonçalves, J., Martins, T., Ferreira, R., Milhazes, N., Borges, F., Ribeiro, C.F., Silva, A.P., 2008. Methamphetamine-Induced Early Increase of IL-6 and TNF-α mRNA Expression in the Mouse Brain. Annals of the New York Academy of Sciences 1139 (1), 103–111.
Guo, H., Ingolia, N.T., Weissman, J.S., Bartel, D.P., 2010. Mammalian microRNAs predominantly act to decrease target mRNA levels. Nature 466 (7308), 835.
Herd, S.A., Banich, M.T., O'reilly, R.C., 2006. Neural mechanisms of cognitive control: an integrative model of Stroop task performance and fMRI data. J. Cogn. Neurosci. 18 (1), 22–32.
Huang, X., Chen, Y., Shen, Y., Cao, X., Li, A., Liu, Q., Tan, T., 2017. Methamphetamine abuse impairs motor cortical plasticity and function. Molecular psychiatry 22 (9), 1274.
Jayanthi, S., Deng, X., Ladenheim, B., McCoy, M.T., Cluster, A., Cai, N.-s., Cadet, J.L., 2005. Calcineurin/NFAT-induced up-regulation of the Fas ligand/Fas death pathway is involved in methamphetamine-induced neuronal apoptosis. Proc. Natl. Acad. Sci. 102 (3), 868–873.
Krebs, R.M., Boehler, C.N., Roberts, K.C., Song, A.W., Woldorff, M.G., 2012. The involvement of the dopaminergic midbrain and cortico-striatal-thalamic circuits in the integration of reward prospect and attentional task demands. Cereb. Cortex (New York, N.Y.: 1991) 22 (3), 607–615. https://doi.org/10.1093/cercor/bhr134.
L. Simon, C.D., Carnell, Jennifer, Brethen, Paul Brethen, Rawson, Richard, Walter Ling, Sara, 2000. Cognitive impairment in individuals currently using methamphetamine. Am. J. Addict. 9 (3), 222–231.
Lamers, K., 2003. Protein S100, NSE, myelin basic protein (MBP), and glial fibrillary acid protein in CSF and blood of neurological patints. Brain Res. Bull. 15 (7), 261–264.
Larsen, K.E., Fon, E.A., Hastings, T.G., Edwards, R.H., Sulzer, D., 2002. Methamphetamine-induced degeneration of dopaminergic neurons involves autophagy and upregulation of dopamine synthesis. J. Neurosci. 22 (20), 8951–8960.
Li, H., Li, C., Zhou, Y., Luo, C., Ou, J., Li, J., Mo, Z., 2018. Expression of microRNAs in the serum exosomes of methamphetamine-dependent rats vs. ketamine-dependent rats. Exp. Ther. Med. 15 (4), 3369–3375.
London, E.D., Kohno, M., Morales, A.M., Ballard, M.E., 2015. Chronic methamphetamine abuse and corticostriatal deficits revealed by neuroimaging. Brain Res. 1628, 174–185.
Marchi, N., Rasmussen, P., Kapural, M., Fazio, V., Kight, K., Mayberg, M.R., Cavaglia, M., 2003. Peripheral markers of brain damage and blood-brain barrier dysfunction. Restorative neurology and neuroscience 21 (3, 4), 109–121.
Moratalla, R., Khairnar, A., Simola, N., Granado, N., García-Montes, J.R., Porceddu, P.F., Morelli, M., 2017. Amphetamine-related drugs neurotoxicity in humans and in experimental animals: main mechanisms. Progress in neurobiology 155, 149–170.
Moszczynska, A., Callan, S.P., 2017. Molecular, behavioral, and physiological consequences of methamphetamine neurotoxicity: implications for treatment. J. Pharmacol. Exp. Ther. 362 (3), 474–488.

Nestor, L.J., Ghahremani, D.G., Monterosso, J., London, E.D., 2011. Prefrontal hypoactivation during cognitive control in early abstinent methamphetamine-dependent subjects. Psychiatry Res. Neuroimaging 194 (3), 287–295.
Ohta, M., Ohta, K., Nishimura, M., Saida, T., 2002. Detection of myelin basic protein in cerebrospinal fluid and serum from patients with HTLV-1-associated myelopathy/tropical spastic paraparesis. Ann. Clin. Biochem. 39 (6), 603–605.
Pubill, D., Canudas, A.M., Pallàs, M., Camins, A., Camarasa, J., Escubedo, E., 2003. Different glial response to methamphetamine-and methylenedioxymethamphetamine-induced neurotoxicity. Naunyn Schmiedeberg's Arch. Pharmacol. 367 (5), 490–499.
Ruan, X., Zhong, N., Yang, Z., Fan, X., Zhuang, W., Du, J., Zhao, M., 2018. Gray matter volume showed dynamic alterations in methamphetamine users at 6 and 12 months abstinence: A longitudinal voxel-based morphometry study. Progress in Neuro-Psychopharmacology and Biological Psychiatry 81, 350–355.
Salo, R., Ursu, S., Buonocore, M.H., Leamon, M.H., Carter, C., 2009. Impaired prefrontal cortical function and disrupted adaptive cognitive control in methamphetamine abusers: a functional magnetic resonance imaging study. Biol. Psychiatry 65 (8), 706–709.
Sekine, Y., Minabe, Y., Ouchi, Y., Takei, N., Iyo, M., Nakamura, K., Yoshikawa, E., 2003. Association of dopamine transporter loss in the orbitofrontal and dorsolateral prefrontal cortices with methamphetamine-related psychiatric symptoms. American Journal of Psychiatry 160 (9), 1699–1701.
Sekine, Y., Ouchi, Y., Sugihara, G., Takei, N., Yoshikawa, E., Nakamura, K., Suzuki, K., 2008. Methamphetamine causes microglial activation in the brains of human abusers. Journal of Neuroscience 28 (22), 5756–5761.
Sen, J., Belli, A., 2007. S100B in neuropathologic states: the CRP of the brain? J. Neurosci. Res. 85 (7), 1373–1380.
Shin, E.-J., Tran, H.-Q., Nguyen, P.-T., Jeong, J.H., Nah, S.-Y., Jang, C.-G., Kim, H.-C., 2018. Role of Mitochondria in Methamphetamine-Induced Dopaminergic Neurotoxicity: Involvement in Oxidative Stress, neuroinflammation, and Pro-apoptosis—A Review. Neurochemical research 43 (1), 57–69.
Stroop, J.R., 1935. Studies of interference in serial verbal reactions. J. Exp. Psychol. 18 (6), 643.
Su, Z., Yang, Z., Xu, Y., Chen, Y., Yu, Q., 2015. MicroRNAs in apoptosis, autophagy and necroptosis. Oncotarget 6 (11), 8474.
Thompson, P.M., Hayashi, K.M., Simon, S.L., Geaga, J.A., Hong, M.S., Sui, Y., London, E. D., 2004. Structural abnormalities in the brains of human subjects who use methamphetamine. Journal of Neuroscience 24 (26), 6028–6036.
Wang, J.-X., Zhang, X.-J., Li, Q., Wang, K., Wang, Y., Jiao, J.-Q., Gong, Y., 2015. MicroRNA-103/107 Regulate Programmed Necrosis and Myocardial Ischemia/Reperfusion Injury Through Targeting FADDNovelty and Significance. Circulation research 117 (4), 352–363.
Wilson, J.M., Kalasinsky, K.S., Levey, A.I., Bergeron, C., Reiber, G., Anthony, R.M., Kish, S.J., 1996. Striatal dopamine nerve terminal markers in human, chronic methamphetamine users. Nature medicine 2 (6), 699.
Worsley, K.J., 2001. 14 statistical analysis of activation images. In: Functional MRI: An Introduction to Methods, p. 251.
Worsley, J., Moszczynska, A., Falardeau, P., Kalasinsky, K., Schmunk, G., Guttman, M., Reiber, G., 2000. Dopamine D1 receptor protein is elevated in nucleus accumbens of human, chronic methamphetamine users. Molecular psychiatry 5 (6), 664.
Xiao, N., Zhang, F., Zhu, B., Liu, C., Lin, Z., Wang, H., Xie, W.-B., 2018. CDK5-mediated tau accumulation triggers methamphetamine-induced neuronal apoptosis via endoplasmic reticulum-associated degradation pathway. Toxicol. Lett. 292, 97–107.
Xiong, K., Liao, H., Long, L., Ding, Y., Huang, J., Yan, J., 2016. Necroptosis contributes to methamphetamine-induced cytotoxicity in rat cortical neurons. Toxicol. in Vitro 35, 163–168.
Yamazaki, Y., Yada, K., Morii, S., Kitahara, T., Ohwada, T., 1995. Diagnostic significance of serum neuron-specific enolase and myelin basic protein assay in patients with acute head injury. Surg. Neurol. 43 (3), 267–271.
Yilmaz, S., Karakayali, O., Kale, E., Akdogan, A., 2018. Could serum S100B be a predictor of neuronal damage and clinical poor outcomes associated with the use of synthetic cannabinoids? S100B to predict neuronal damage of SC in the ED. Am. J. Emerg. Med. 36 (3), 435–441.
Yin, R., Lu, C., Chen, Q., Fan, J., Lu, J., 2013. Microvascular damage is involved in the pathogenesis of heroin induced spongiform leukoencephalopathy. Int. J. Med. Sci. 10 (3), 299.
Yu, S., Zhu, L., Shen, Q., Bai, X., Di, X., 2015. Recent advances in methamphetamine neurotoxicity mechanisms and its molecular pathophysiology. Behav. Neurol. 2015.
Zhang, J., Sun, X., Zheng, S., Liu, X., Jin, J., Ren, Y., Luo, J., 2014. Myelin basic protein induces neuron-specific toxicity by directly damaging the neuronal plasma membrane. PLoS One 9 (9), e108646.
Zhao, Y., Zhang, K., Jiang, H., Du, J., Na, Z., Hao, W., Zhao, M., 2016. Decreased expression of plasma microRNA in patients with methamphetamine (MA) use disorder. Journal of Neuroimmune Pharmacology 11 (3), 542–548.
Zhong, N., Jiang, H., Du, J., Zhao, Y., Sun, H., Xu, D., Hashimoto, K., 2016. The cognitive impairments and psychological wellbeing of methamphetamine dependent patients compared with health controls. Progress in Neuro-Psychopharmacology and Biological Psychiatry 69, 31–37.